Guy Bessonnet
Stéphane Chessé
Philippe Sardain

Laboratoire de Mécanique des Solides, CNRS-UMR6610
University of Poitiers, SP2MI, Bd. M. & P. Curie, BP 30179
86962 Futuroscope-Chasseneuil, France
bessonnet@lms.univ-poitiers.fr

Optimal Gait Synthesis of a Seven-Link Planar Biped

Abstract

In this paper, we carry out the dynamics-based optimization of sagittal gait cycles of a planar seven-link biped using the Pontryagin maximum principle. Special attention is devoted to the double-support phase of the gait, during which the movement is subjected to severe limiting conditions. In particular, due to the fact that the biped moves as a closed kinematic chain, overactuation must be compatible with double, non-sliding unilateral contacts with the supporting ground. The closed chain is considered as open at front foot level. A full set of joint coordinates is introduced to formulate a complete Hamiltonian dynamic model of the biped. Contact forces at the front foot are considered as additional control variables of the stated optimal control problem. This is restated as a state-unconstrained optimization problem which is finally recast, using the Pontryagin maximum principle, as a two-point boundary value problem. This final problem is solved using a standard computing code. A gait sequence, comprising starting, cyclic, and stopping steps, is generated in the form of a numerical simulation.

KEY WORDS—sagittal gait, gait optimization, Pontryagin maximum principle

1. Introduction

Walking is an essentially unstable movement. It requires perfect coordination of joint actuating torques, together with accurate control of ground reaction forces in order to ensure the dynamic balance of the biped. Therefore, mastering such a movement requires mastering its dynamics.

The most popular technique used to generate and control a stable gait is based on the concept of "zero moment point" (ZMP) presented in Vukobratovic et al. (1990). It was especially used in Hirai, Hirose, and Takenaka (1998), Fujimoto, Obata, and Kawamura (1998), Inoue et al. (2000) and Löffler,

Gienger, and Pfeiffer (2002) to control the gait of humanoid robots walking on a level surface. The ZMP correlates the motion dynamics with the normal contact forces exerted on level ground. In this case, the normal forces are reducible to a unique force applied to a point of the supporting surface where their moment is zero. This point is the center of pressure (CoP) which coincides with the ZMP. If the CoP–ZMP migrates to the edge of the supporting surface (in fact the convex hull of all supporting surfaces) the biped may be precariously balanced and even lose its equilibrium. Thus, the ZMP criterion is a rather simple and efficient means of controlling the gait of a walking machine. However, this technique makes use of a global dynamic model and does not allow the internal motion organization to be taken directly into account. A different strategy, based on a control parameter optimization approach, is presented in Kiriazov (2002). It allows for the adjusting of a finite set of control parameters in order to satisfy output conditions and minimize an energy cost. The method is applied to the gait synthesis of a seven-link planar biped.

Another approach is to develop numerical motion generators for computing reference trajectories that are kinematically well organized and dynamically stable, respecting the intrinsic dynamics of the biped. This idea results in extracting, using an appropriate selecting criterion, a solution of the motion equations fitting the biped capacities at best, as well as satisfying kinematic and sthenic constraints that define a feasible gait. In this way, a motion optimization problem is stated whereby reference steps are generated by minimizing a performance criterion on a double set of feasible control and state variables. The movements generated, having improved kinematics and dynamics, are anticipated to be easier to control and less energy-consuming.

Essentially two quite different methods have been developed to generate optimal gait trajectories. The most frequently used approach is based on parametric optimization, whereas the second comes within the framework of optimal control theory. Parametric optimization techniques developed for the purpose of motion optimization mostly rely on representing

the joint trajectories or any equivalent set of variables as functions of time defined by a finite set of discrete parameters to be dealt with as optimization variables. The nonlinear optimization problem that results can be solved by implementing sequential quadratic programming algorithms, widely used in the field of mathematical programming. Early attempts to generate optimal steps of five-link bipeds using this approach were carried out in Beletskii and Chudinov (1977) and Channon, Hopkins, and Pham (1992) using polynomial functions defined over the whole range of time. The single-support phase (SSP) only is considered, as in Chevallereau and Aoustin (2001) and Plestan et al. (2003), where a sagittal gait cycle consists of a swing phase ending with an instantaneous impact, this initiating the following step. In Muraro, Chevallereau, and Aoustin (2003) a similar approach is used to generate three different gaits of a quadruped considered as three different bipeds by putting symmetric legs together. Unlike for the above works, in Saidouni and Bessonnet (2003) cubic splines connected at points uniformly distributed along the motion time are used to generate complete optimal steps, including a double-support phase (DSP). We can also mention Martin and Bobrow (1999) where B-splines were used to approximate the joint trajectories of open kinematic chains. The authors emphasized the need for using analytic gradients of the cost functions and constraints. Accordingly, in Section 2 of this paper, we emphasize the need to use exact formulation of Jacobians and gradients in order to cope with the stiff numerical conditioning of the stated problems.

Parametric optimization is an efficient means for computing suboptimal trajectories. However, due to the fact that discrete optimization variables are reduced to a finite number, the complete fulfillment of constraints, defined over the whole range of time, may be difficult to achieve. Besides, polynomial functions may introduce undesirable oscillations of approximated functions (Visioli 2000) or jerky variations of the same functions at connecting points (Saidouni and Bessonnet 2002).

In the second method, the optimization problem is considered as an optimal control problem to be dealt with using the Pontryagin maximum principle (PMP). As shown in Bessonnet, Sardain, and Chessé (2002), a major interest in using the PMP lies in its ability to account directly and exactly for limitations and constraints affecting kinetic loads, actuating inputs and contact forces. In a similar way, state constraints, set in order to limit joint motions and avoid obstacles, can be uniformly satisfied. However, the PMP is often perceived as being computationally ineffective. It should be emphasized that its computational effectiveness is revealed by employing Hamiltonian dynamic models (Bessonnet, Sardain, and Chessé 2002).

A first attempt to generate optimal walk was formally carried out using the PMP in Chow and Jacobson (1971). Recently, in Rostami and Bessonnet (2001), the SSP of a planar seven-link biped was optimized by considering a limited set of independent joint coordinates. A complete cyclic step involving SSPs and DSPs of a footless five-link biped was generated in Chessé and Bessonnet (2001).

The main objective of this work is to solve the constrained-dynamics problem which arises during the DSP of gait, a planar biped having human-like feet being considered. Generating this crucial phase of gait will help in the creation of walking sequences involving starting, cyclic, decelerating, and stopping steps. Furthermore, generating SSPs without impact at heel-touch will ensure the continuity of velocities throughout any gait sequence. Such an objective is aimed at providing the local controller of the robot with reference movements that are well coordinated, dynamically efficient, and low on energy consumption.

The present paper extends and deepens the study presented in Bessonnet, Chessé, and Sardain (2002). The presentation is focused on the DSP. During this, the locomotion system works as a planar seven-bar mechanism subjected to unilateral contacts with its supporting base. The basic idea consists of freeing a ground–foot contact in order, first, to deal with a full set of configuration variables and, second, to consider contact forces as additional actuating control variables giving direct control over their limiting values.

In Section 2, the kinematic model of the seven-link planar model of the biped robot BIP described in Sardain, Rostami, and Bessonnet (1998) and Espiau and Sardain (2000) is thoroughly detailed. In Section 3, attention is focused on the constrained Hamiltonian dynamic model to be dealt with in the DSP, during which the biped moves as a closed kinematic chain. Constraints defining a feasible step are formulated in Section 4. In Section 5, a constrained optimization problem is recast as a state-unconstrained optimal control problem. Applying the PMP in Section 6 allows the latter problem to be solved as a two-point boundary value problem. Section 7 is devoted to the presentation of numerical simulations including generations of starting, cyclic, decelerating, and stopping steps. Conclusions and prospects are formulated in Section 8.

2. Kinematic Model of the Planar Biped

In this section, the walking cycle of sagittal human-like gait is described mainly for the purpose of dynamic modeling. We can recall that, for orthopedists, the typical walk cycle is the stride which refers to the motion cycle of either locomotion limb. Conventionally, it goes from the foot strike of one limb to the next foot strike of the same limb (Sutherland, Kaufman, and Moitoza 1994). In human locomotion, this kinematic scheme is perfectly appropriate for analyzing normal and pathological walking, considering either limb during its own cycle. A different scheme is needed to accomplish the dynamic modeling of the gait. In this case, since the simultaneous driving effects of both legs must be taken into account, the gait has to be considered as a sequence of steps. Steps can
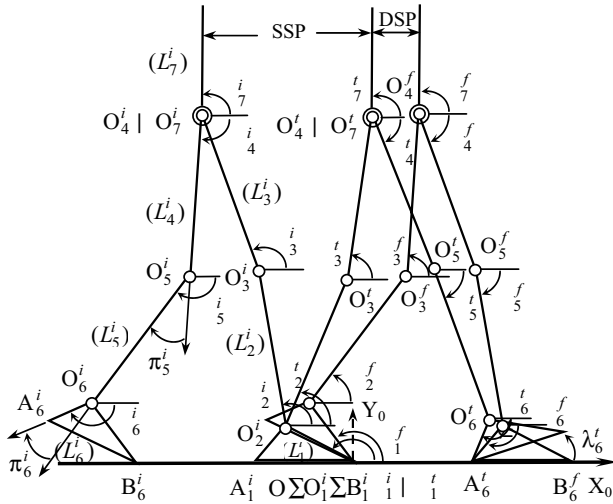
Fig. 1. Cyclic step of a planar seven-link biped; equalities $L^i = \left| B_6^i B_1^i \right| = L^f = \left| B_1^i B_6^f \right|$ define the step length.

be executed in quite varied ways, while showing kinematic features which are fundamentally the same. In particular, any step is the result of linking two successive phases, kinematically quite different (Figure 1).

- The SSP, during which the locomotion system moves as an open tree-like kinematic chain. This motion has the greater amplitude. It goes from toe-off to heel-touch of the foot of the swing leg.

- The DSP, during which the locomotion system is kinematically closed, and overactuated. It goes from heel-touch of the front foot to toe-off of the rear foot. It can be considered as a movement of propulsion and equilibrium recovery. Its amplitude is less than the SSP.

It must be emphasized that the notion of closed kinematics needs to take very restricting conditions into account for stating and dealing with dynamic models of mechanical systems having kinematic loops. These conditions are even more constraining when considering closure statements due to unilateral contacts. This is the situation in the case of the double support of gait.

The kinematic configuration of the biped may change during each of both above phases. In particular, the DSP comprises an initial heel rocker movement of the front foot followed by foot-flat contact. The latter subphase results in the loss of one degree of freedom with respect to the initial configuration. On the other hand, in Figure 1, the whole SSP is represented with flat contact of the stance foot. This kinematic choice may be considered as suitable for a mechanical biped. However, during human gait, the stance foot rotates

about its metatarsal axis before toeing-off. This additional joint motion generates a subphase whose kinematic configuration introduces one further degree of freedom. In this case, the joint configuration of the planar biped model changes from six degrees of freedom to seven.

By contrast, the presence of a kinematic loop results in the reduction of the number of degrees of freedom of the locomotion system: two and three degrees of freedom are lost in the sagittal model before and after the front foot is flat on the ground, three and six, respectively, for a three-dimensional biped, assuming that heel contact acts as a single point on the ground before the foot becomes flat. This double cut in the number of degrees of freedom could suggest that the configuration variables should be reduced to a set of independent joint coordinates. Such a transformation would require expressing the remaining joint coordinates as functions of independent ones. As the total number of joint coordinates is large, this operation would be quite involved. Furthermore, it would lead to impractical formulations of motion equations. To avoid such intricacy, we need to model the biped as an open kinematic chain during the DSP.

In the course of the sequence of events SSP–DSP shown in Figure 1, the tip of the foot located in middle position (point B_1^i) is a fixed fulcrum about which the foot rotates (or does not rotate in the case of the beginning of SSP) with respect to the ground. It is then practical to consider this central foot as the proximal link L_1 of the planar biped, and to describe the joint motions successively (as indicated in Figure 1) for the other foot, now labeled L_7 and considered as the distal link. Then the same set of joint coordinates (consisting, for instance, of absolute joint rotations defined as indicated in Figure 1) may be used to describe both SS and DS phases. Note that the complementary sequence DSP–SSP would not allow such a common description of the two step phases.

In the above kinematic description, it is assumed that the kinematic loop formed by the locomotion system during the DSP is cut at the level of ground contact of the front foot, labeled L_6^f in Figure 1. In this way, in both phases, the same n_q-order coordinate-vector, defined as

$$\mathbf{q} = (q_1, ..., q_{n_q})^T, \quad q_i \equiv \theta_i, \quad i \leqslant n_q, \quad n_q = 7, \quad (1)$$

will be used to formulate the motion equations of the biped.

The step cycle is characterized by limiting postural configurations identified in Figure 1 by the superscripts "i" standing for initial (configuration), "t" for transition (between SSP and DSP), and "f" for final. The first coordinate q_1 will be assumed to remain constant during the SSP, namely

$$t \in [t^i, t^t], \quad q_1(t) = \pi - \beta, \quad (2)$$

while in the DSP, the vector $\boldsymbol{q}$ in eq. (1) is subjected to closure constraints that can be written as (see Figure 1 for the notations)
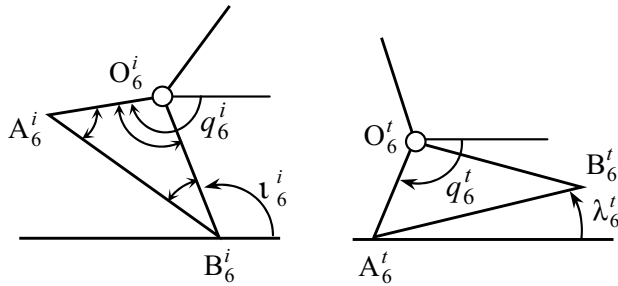
Fig. 2. Rear foot at toe-off, and front foot at heel-touch.

$$t \in [t^t, t^f], \quad \begin{cases} C_1(\mathbf{q}(t)) \equiv O_1^i A_6^t \cdot X_0 - L + \ell = 0, & (3) \\ C_2(\mathbf{q}(t)) \equiv O_1^i A_6^t \cdot Y_0 = 0, & (4) \end{cases}$$

$$\in [t^t + \varepsilon, t^f], \quad C_3(\mathbf{q}(t)) \equiv \phi(\mathbf{q}(t)) = 0. \tag{5}$$

In eq. (2), β is the angle of the foot triangle at the tip B_6^i (Figure 2).

Constraints C_1 and C_2 in eqs. (3) and (4) specify the Cartesian coordinates of the contact point A_6^t of the heel of the front foot. In eq. (3), L and ℓ denote the step and foot lengths, respectively. In eq. (5), ϕ represents the inclination angle of the front foot with the ground; ε is a short duration, after which the front foot remains flat on the ground, as specified by the constraint C_3.

In the following, constraints such as eqs. (3), (4), and (5) will be put together in the vector-valued function $\mathbf{C}^h$ defined as

$$\mathbf{C}^h(\mathbf{q}) = (C_1(\mathbf{q}), ..., C_{n_h}(\mathbf{q}))^T, \tag{6}$$

where n_h is the number of closure (or holonomic) constraints ($n_h = 2$ or 3, above).

Moreover, the Jacobian matrix

$$\mathbf{\Phi}(\mathbf{q}) = \partial \mathbf{C}^h / \partial \mathbf{q} \tag{7}$$

is used in the next section for deriving the Lagrange equation of motion.

Another approach could be used to describe the closed kinematics of the biped. Some authors, such as Azevedo, Poignet, and Espiau (2002), Chevallereau and Aoustin (2001) and Saidouni and Bessonnet (2003), cut all ground contacts and consider the biped as a free system in the two-dimensional Cartesian space. The Cartesian coordinates of the hip point are added to the seven joint coordinates to describe the biped motions. Two or three further closure conditions formulated at the rear foot level are added to the above constraints (2)–(5). The main interest of this description lies in the fact that it allows the formulation of motion equations to be identical for the two step phases. Nevertheless, the approach described below leads to a less constrained problem that is also simpler to formulate.

Absolute joint coordinates defined in Figure 1 lead to the formulation of a concise dynamic model. No three-dimensional model of the biped would benefit from this simpler description. In this case, introducing a set of relative joint coordinates, defined for instance using the well-known Denavit–Hartenberg construction, becomes necessary.

3. Constrained Dynamic Model

As we want to formulate motion equations using a full set of dependent configuration variables, this approach will result in proposing a constrained dynamic model. Moreover, as we intend to implement the PMP, a state equation formulated in state space form is required. Special attention is devoted to both the above dynamic modeling aspects in the following subsections.

3.1. Basic Dynamic Formulation

As stated in Section 2, in both motion phases the biped is assumed to be an open kinematic chain, the front foot contact being explicitly specified through closure constraints. This kinematic description results in stating a Lagrangian dynamic model with Lagrange multipliers, subjected to geometric closure conditions, i.e., holonomic constraints. Lagrange equations may be formulated as the general n_q-vector equation

$$\mathbf{M}(\mathbf{q})\ddot{\mathbf{q}} + \mathbf{C}(\mathbf{q}, \dot{\mathbf{q}}) + \mathbf{G}(\mathbf{q}) = \mathbf{D}(\mathbf{q}, \dot{\mathbf{q}}) + \mathbf{B}\,\boldsymbol{\tau} + \mathbf{\Phi}^T(\mathbf{q})\boldsymbol{\lambda}, \tag{8}$$

where M is the biped mass-matrix, C contains centrifugal and Coriolis inertia terms, G and D represent gravity and dissipative terms, respectively, $\boldsymbol{\tau}$ is the n_q-vector of actuating joint torques, defined as $\boldsymbol{\tau} = (0, \tau_2, ..., \tau_{n_q})^T$ ($\tau_1 = 0$ means that, unlike the human foot, the tip of the foot is not actuated), $\boldsymbol{\lambda}$ is the Lagrange n_h-vector multiplier associated to holonomic constraints $\mathbf{C}^h$, and B is a matrix that depends on the choice of joint coordinates.

Equation (8) is the basic dynamic model we need to begin with. In fact, this equation cannot be dissociated from constraints (6) (or, equivalently, constraints (3)–(5)). This double system of relationships is a set of differential-algebraic equations. As discussed in Chessé and Bessonnet (2001) it needs to be especially adapted for implementing the PMP. With this aim in view, a first requirement is to restate the Lagrange equations in Hamiltonian form.

3.2. Hamiltonian Dynamic Model

Hamiltonian formalism is not in widespread use in the field of multibody system dynamics. Nevertheless, as shown in

Bessonnet, Sardain, and Chessé (2002), a dynamic state equation formulated in Hamiltonian canonic variables has a mathematical structure that is perfectly appropriate for implementing the PMP, that is to say for deriving the necessary optimality conditions stated by the maximum principle itself.

The reader is referred to Bessonnet, Sardain, and Chessé (2002) for specific statements related to Hamiltonian dynamic equations. In brief, we can recall that they are derived from the Lagrange equations by means of a change of variables that consists of substituting the conjugate momentum $\mathbf{p} = \partial T/\partial \dot{\mathbf{q}}$ (the Legendre transformation, where T is the kinetic energy of the mechanical system) for the Lagrangian velocity $\dot{\mathbf{q}}$. Then it can be shown (Bessonnet, Sardain, and Chessé 2002) that the Lagrangian vector-equation (8) splits up into two n_q-order subsystems solved in the Hamiltonian phase velocities $(\dot{\mathbf{q}}, \dot{\mathbf{p}})$ as follows

$$\begin{cases} \dot{\mathbf{q}} = \mathbf{M}^{-1}(\mathbf{q})\mathbf{p} \equiv \mathbf{g}(\mathbf{q}, \mathbf{p}), \\ \dot{\mathbf{p}} = \frac{1}{2}\mathbf{g}^T\mathbf{M}_{,\mathbf{q}}\mathbf{g} - \mathbf{G}(\mathbf{q}) + \mathbf{D}(\mathbf{q}, \mathbf{g}(\mathbf{q}, \mathbf{p})) + \mathbf{B}\boldsymbol{\tau} + \mathbf{\Phi}^T(\mathbf{q})\boldsymbol{\lambda}, \end{cases}$$
$$(9)$$

where $\mathbf{M}_{,q} \equiv \partial\mathbf{M}/\partial\mathbf{q}$.

At this point, two types of variables must be identified, as follows.

- The state variables of the controlled mechanical system, which are simply the Hamiltonian phase variables (or canonic variables) q and p that we put together in the $2n_q$-vector x such as $\mathbf{x}^T = (\mathbf{q}^T, \mathbf{p}^T)$.

- The control variables, which are the joint actuating torques. However, the multiplier $\boldsymbol{\lambda}$ represents efforts to be applied to the front foot in order to hold this foot in its specified ground-contact position. Thus, it is possible to add the components of $\boldsymbol{\lambda}$ as complementary control variables. In this way, we are able to exert direct control over the contact forces. These must obey specific conditions, as stated in Section 4.3. Consequently, we define the control vector on each phases by setting

$$t \in [t^i, t^t], \quad \bar{\mathbf{u}}(t) = \boldsymbol{\tau}(t) \tag{10}$$

$$t \in [t^t, t^f], \quad \mathbf{u}(t)^T = (\boldsymbol{\tau}(t)^T, \boldsymbol{\lambda}(t)^T). \tag{11}$$

Equations (9) may be then restated on the first interval of time as the $2n_q$-order differential equation

$$t \in [t^i, t^t], \quad \dot{\mathbf{x}}(t) = \bar{\mathbf{f}}(\mathbf{x}(t)) + \mathbf{B}\,\bar{\mathbf{u}}(t) \equiv \bar{\mathbf{F}}(\mathbf{x}(t), \bar{\mathbf{u}}(t)), \tag{12}$$

while, on the second, we have to deal with the differential-algebraic system

$$t \in [t^t, t^f], \quad \begin{cases} \dot{\mathbf{x}}(t) = \mathbf{f}(\mathbf{x}(t)) + \mathbf{B}^*(\mathbf{x}(t))\mathbf{u}(t) \\ \quad \equiv \mathbf{F}(\mathbf{x}(t), \mathbf{u}(t)), \tag{13} \\ \mathbf{C}^h(\mathbf{x}(t)) = \mathbf{0}, \tag{14} \end{cases}$$

where $\mathbf{B}^*(\mathbf{x}) \equiv (\mathbf{B}, \mathbf{\Phi}^T(\mathbf{x}))$.

Both state equations (12) and (13) have the required form to implement the PMP. We emphasize the fact that the Jacobian matrix $\partial\mathbf{F}/\partial\mathbf{x}$ of F in eq. (13) must be derived exactly, in order to benefit from accurate computation of the associated adjoint system (45). This results from the implementation of the PMP, as shown below.

4. Defining a Feasible Step

Any feasible step obeys some specified conditions and limits the way we define a realistic gait which the biped will be able to execute efficiently and control safely. Such specifications defined on the step cycle may be instantaneous or continuous. Also, they can apply to phase variables, as well as to control inputs.

The first basic data to be introduced are the walk speeds, V. The step length, L, may be specified or optimized versus V. In any case, the step cycle time $T = t^f - t^i$ is defined by the relationship $T = L/V$. Moreover, setting $T_{SS} = t^t - t^i$ and $T_{DS} = t^f - t^t$, we consider that the DSP time represents about 0.15%–0.25% of the cycle time as observed in human walking, i.e.,

$$T_{DS} = T - T_{SS} = k\,T\,, 0.15 \leqslant k \leqslant 0.25.$$

4.1. Transition Constraints

These are instantaneous constraints that characterize or define transition postural configurations between the step phases. In Figure 1, the SSP–DSP cycle is depicted by three limiting configurations identified using superscripts i, t, and f, as already mentioned in Section 2. The step pattern is essentially defined by feet and hip positions and velocities at transition times t^i, t^t, and t^f.

At initial time t^i, the position and velocity of the tip B_6^i of the rear foot at toe-off must satisfy

$$\text{OB}_6^i = -L^i\,\mathbf{X}_0, \mathbf{V}(B_6^i) = 0 \tag{15}$$

where L^i is the initial step length, while V is the velocity vector.

It can be noted that many authors take into account heel-strike and introduce an equation of impact at transition between successive steps (see, for example, Channon, Hopkins, and Pham 1992; Chevallereau and Aoustin 2001; Plestan et al. 2003). This means that velocities are discontinuous and subjected to instantaneous jumps from one step to the other. Such a condition implies that accelerations have infinite jumps. At transition time t^t, this situation is avoided here, since we specify, as advocated in Blajer and Schiehlen (1992), impactless heel-touch at point A_6^t in order to prevent destabilizing effects

on the motion control of the biped. Conditions to be satisfied are similar to constraints (15), namely

$$OA_6^t = (L^f - \ell)\mathbf{X}_0, \quad \mathbf{V}(A_6^t) = 0, \qquad (16)$$

where L^f is the final step length, and ℓ is the foot length.

At final time t^f, the front foot being considered as flat on the ground, we must have

$$OO_6^f = OO_6^i + L^f\mathbf{X}_0, \quad \mathbf{V}(O_6^f) = 0. \qquad (17)$$

Projecting the above six vector-relationships on ortho-normalized base vectors $\mathbf{X}_0$ and $\mathbf{Y}_0$ yields scalar relationships, which we write formally as

$$k \leqslant n_{tc}, \quad \begin{cases} C_k^i(\mathbf{x}_L(t^i)) = 0, & (18) \\ C_k^t(\mathbf{x}_L(t^t)) = 0, & (19) \\ C_k^f(\mathbf{x}_L(t^f)) = 0, & (20) \end{cases}$$

where $\mathbf{x}_L$ is the vector of the Lagrange phase variables, $\mathbf{x}_L^T = (\mathbf{q}^T, \dot{\mathbf{q}}^T)$, and n_{tc} is here equal to 4.

If the step is cyclic, first $L^f = L^i = L$ and, secondly, $\mathbf{x}_L(t^f)$ must be identified to $\mathbf{x}_L(t^i)$, given that the legs are switched. Using the joint coordinate representation in Figure 1, correlations between $\mathbf{x}_L(t^f)$ and $\mathbf{x}_L(t^i)$ result from exchanging initial and final coordinates as follows

$$\begin{aligned} q_1^f &= q_6^i + \gamma + \pi, \; q_2^f = q_5^i + \pi, \; q_3^f = q_4^i + \pi \\ q_4^f &= q_3^i - \pi, \; q_5^f = q_2^i - \pi, \; q_6^f = -\beta - \gamma, \; q_7^f = q_7^i \end{aligned}$$
$$(21)$$

and swapping the joint velocities according to the scheme

$$k \leqslant 5, \quad \dot{q}_k^f = \dot{q}_{7-k}^i, \quad \dot{q}_6^f = 0, \; \dot{q}_7^f = \dot{q}_7^i. \qquad (22)$$

Let us note that the relationships in eq. (22) appear simply as the derivatives of relationships (21). Moreover, in that case, due to eqs. (21) and (22), constraints (20) are ipso facto satisfied.

Further conditions must be added to constraints (18)–(20) in order to ensure step feasibility. We have a choice between two approaches. The first approach would be to limit the values of key factors such as position and velocity of hip joint, inclination, and rotation rate of the trunk, and feet at toe-off and heel-touch. Such an approach would allow the transition states $\mathbf{x}_L(t^i)$, $\mathbf{x}_L(t^t)$, and $\mathbf{x}_L(t^f)$ to be optimized while accounting for constraints (18)–(20). A simpler approach would be to specify the above factors as follows (see Figures 1 and 2 for notations and symbols)

$$k = i, \; t, \; f \quad \begin{cases} OO_4^k \cdot \mathbf{X}_0 = X_4^k, \; OO_4^k \cdot \mathbf{Y}_0 = Y_4^k \\ \mathbf{V}(O_4^k) \cdot \mathbf{X}_0 = V_{4X}^k, \; \mathbf{V}(O_4^k) \cdot \mathbf{Y}_0 = V_{4Y}^k \\ q_7^k \cong \pi/2, \; \dot{q}_7^k \cong 0 \end{cases}$$
$$(23)$$

$$\begin{aligned} q_6^i &= \delta_6^i - \gamma - \pi, \; \dot{q}_6^i = \omega_6^i \\ q_6^t &= \phi_6^t + \alpha - \pi, \; \dot{q}_6^t \cong 0 \qquad (24) \\ q_1^f &= \delta_1^f, \; \dot{q}_1^f = \omega_1^f \end{aligned}$$

where quantities in the right-hand terms denote given values. The symbol "$\cong$" means that these values might be slightly different from indicated ones. Then, relationships (18)–(20) can be solved in $\mathbf{x}_L(t^i)$, $\mathbf{x}_L(t^t)$, and $\mathbf{x}_L(t^f)$. In this way, transition states are known and considered as simple boundary value conditions. In Section 7, numerical simulations are performed using this approach.

4.2. State Constraints

As for any human movement or robot motion, joint trajectories of walking machines must be subjected to a limited range in order to avoid unfeasible movements, such as joint counter-flexion, or ground and obstacle collisions. Such necessary constraints cannot be omitted. They involve joint coordinates and velocities considered throughout the cycle time. Considering relative joint coordinates defined as (Figure 1)

$$\varphi_1 = \theta_1, \varphi_i = \theta_i - \theta_{i-1}, \; i = 2, ..., n_q,$$

joint motion limitations and counter-flexing avoidance at knee and ankle level must be taken into account by setting

$$t \in [t^i, t^f], \quad \begin{cases} \varphi_5^{min} \leqslant \varphi_5(t) \leqslant 0 \\ -\gamma \leqslant \varphi_6(t) \leqslant 0 \\ 0 \leqslant \varphi_3(t) \leqslant \varphi_3^{max} \end{cases}. \qquad (25)$$

The first two double inequalities relate to the knee and ankle of the swing leg. The third refers to the knee of the stance leg, which becomes the rear leg during the DSP. We can rewrite the six above inequalities in the generic form

$$t \in [t^i, t^f], \; C_j^S(\mathbf{x}(t)) \leqslant 0, \; j = 1, ..., 6. \qquad (26)$$

Let us note that joint velocities could be moderated using similar inequalities.

Further constraints must be stated to enable swing foot clearance from the ground, and stepping over an obstacle, if needed. In Figure 3, bell-shaped curves are used to define exclusion zones from which the foot must be removed upwards.

The lower curve may be used for specifying foot clearance, and the upper one for obstacle avoidance. This approach was first introduced in Rostami and Bessonnet (2001). Here, we use a simpler algebraic description of the curve by considering the fourth-order polynomial function

$$x \in [a, b], \; f(x) = h\left(\frac{(x-a)(b-x)}{(c-a)(b-c)}\right)^2$$

where a and b represent the abscissa of points situated between, or coinciding with, the toe-off point B_6^i and the heel-touch point A_6^t. The function f satisfies obviously $f(a) =$
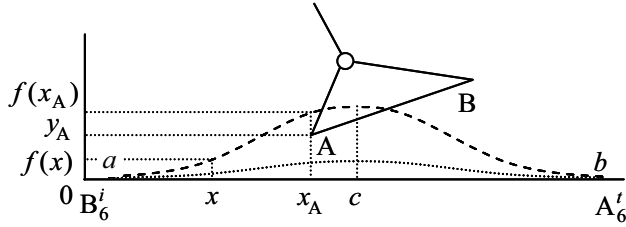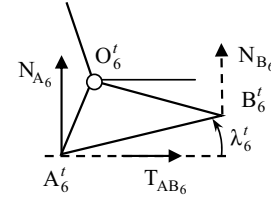
Fig. 3. Foot clearance and obstacle avoidance.

Fig. 4. System of two and three forces exerted on the front foot, equivalent to the ground contact forces. The dotted-line vector N_{B_6} is applied only after the foot is flat on the ground, then $\phi_6^t = 0$.

$f(b) = 0$, $f(c) = h$, $f'(a) = f'(b) = 0$, and $f'(c) = 0$, provided that $c = (a + b)/2$. Therefore, h defines the maximum clearance height. This need only be a few centimeters for walking on level ground. Foot clearance is considered to be effective if the foot sole remains clear of the curve. Fulfillment of this condition by sole ends A and B may be sufficient to prevent any ground collision. Using the notations in Figure 3, such a condition is expressed by the set of inequalities

$$f(x_A) - y_A \leqslant 0, f(x_B) - y_B \leqslant 0$$

where x_A, x_B, y_A, and y_B must be formulated as functions of the state variables, reduced here to the joint coordinates. It is then possible to restate the above constraints in a form similar to eq. (21), i.e.,

$$t \in [t^i, t^t], \ C_j^S(\mathbf{x}(t)) \leqslant 0, \ j = 7, 8. \tag{27}$$

A third constraint formulated for the middle point of the sole might be added to improve the fulfillment of clearance condition.

4.3. Sthenic Constraints

We use the term sthenic constraints (sthenic is from Greek *sthenos* meaning "force"), for restrictions formulated on active and passive interacting forces that are at work and at stake in the kinematic chain. First, technological limitations of actuators need to keep actuating torques within limits such that

$$t \in [t^i, \ t^f], \ \tau_i^{min} \leqslant \tau_i(t) \, (\equiv u_i(t)) \leqslant \tau_i^{max}, \ i = 2, ..., 7. \tag{28}$$

Secondly, contact forces between the biped and the ground must satisfy unilaterality of contact together with non-sliding conditions. Figure 4 shows a way of representing such forces according to whether the foot exerts a single point contact or lies flat on the ground.

At front foot level, the equivalence between these forces and the Lagrange multipliers appearing in eq. (7), and correlated to closure constraints (3)–(5), is as follows

$$(\lambda_1, \ \lambda_2, \ \lambda_3) = (T_{AB_6}, N_{A_6} + N_{B_6}, \ell N_{B_6}) \tag{29}$$

where $N_{B_6} = 0$ for $t \in [t^t, t^t + \varepsilon]$.

Contact constraints to be fulfilled at front foot level are

$$t \in [t^t, t^t + \varepsilon], \ N_{A_6} > 0, \ \left| T_{AB_6} \right| < f N_{A_6} \tag{30}$$

$$t \in [t^t + \varepsilon, t^f], N_{A_6} > 0, \ N_{B_6} > 0,$$
$$\left| T_{AB_6} \right| < f(N_{A_6} + N_{B_6}). \tag{31}$$

In eqs. (30) and (31), positivity of normal forces means that the contact is unilateral. Non-sliding conditions are expressed by the remaining inequalities where f denotes a dry-friction coefficient between the foot sole and the ground.

As suggested by eq. (11), if we set $(\lambda_1, \lambda_2, \lambda_3) = (u_8, u_9, u_{10})$, constraints equivalent to non-sliding conditions in eqs. (30) and (31), in terms of complementary control variables u_i, may be written as

$$t \in [t^t, t^t + \varepsilon], \ \begin{cases} 0 < u_9(t) \\ |u_8(t)| < f u_9(t) \end{cases} \tag{32}$$

$$t \in [t^t + \varepsilon, t^f], \ \begin{cases} 0 < u_{10}(t) < \ell u_9(t) \\ |u_8(t)| < f u_9(t) \end{cases} . \tag{33}$$

Constraints similar to eqs. (30) and (31) must be fulfilled at stance foot level during the SSP, and at rear foot of the DSP.

5. Stating a State-Unconstrained Optimal-Control Problem

Stating the dynamics-based optimization problem we have in mind involves all constraints formulated above, including the motion equation. The performance criterion to be minimized is the essential statement remaining to be formulated.

5.1. Performance Criterion

Generating an optimal movement is fundamentally based on minimizing the amount of effort or energy required to create

the motion. The energy criterion presents some disadvantages. First, resulting optimal actuating torques have discontinuous variations of bang-zero-bang type (see, for example, Lewis and Syrmos 1995). The consequences would be movements executed with repeated backlashes on the joint axis. This could have destabilizing effects on the biped control. Secondly, due to the abovementioned discontinuities, the problem is non-smooth and cannot be solved satisfactorily. A performance criterion, defined as the integral quadratic amount of driving torques τ_i and reaction forces λ_j, represents a suitable choice for dealing with optimal dynamics of jointed multibody systems which have closed kinematics. Thus, we consider the double criterion (with notations from eqs. (10) and (11))

$$J_{SS}(\bar{\mathbf{u}}) = \frac{1}{2} \int_{t^i}^{t^t} \bar{\mathbf{u}}(t)^T \mathbf{D}_{\bar{u}} \bar{\mathbf{u}}\,(t)\,dt \equiv \frac{1}{2} \int_{t^i}^{t^t} \boldsymbol{\tau}(t)^T \mathbf{D}_\tau \boldsymbol{\tau}(t)\,dt$$

(34)

$$J_{DS}(\mathbf{u}) = \frac{1}{2} \int_{t^t}^{t^f} \mathbf{u}\,(t)\mathbf{D}_u\,\mathbf{u}\,(t)dt$$

$$\equiv \frac{1}{2} \int_{t^t}^{t^f} (\boldsymbol{\tau}(t)^T \mathbf{D}_\tau \boldsymbol{\tau}(t) + \boldsymbol{\lambda}(t)^T \mathbf{D}_\lambda \boldsymbol{\lambda}(t))\,dt. \qquad (35)$$

In eqs. (34) and (35), $\mathbf{D}_\tau$ and $\mathbf{D}_\lambda$, or equivalently $\mathbf{D}_{\bar{u}}$ and $\mathbf{D}_u$, are diagonal weighting matrices. Initially, only unity matrices are considered. Then, if we want the optimization process to give more (less) input to torques τ_i, or interacting forces λ_j, the corresponding weighting coefficients will be set at values smaller (greater) than unity. The effect expected can only be revealed by carrying out numerical tests. Values between 0.5 and 2 could be sufficient for producing results showing significant differences.

Minimizing the quadratic values of actuating torques ensures their continuity. Moreover, the biped being essentially subjected to gravity forces, such a criterion will favor upright walking patterns which require little effort to support the biped weight. The quadratic term in λ is aimed at minimizing antagonistic forces, especially sliding forces, which might appear in the locomotion system during the DSP.

Bounds introduced in eq. (28) on control variables $\tau_i(i \leqslant n_\tau = 7)$ define, during the SSP, a set of feasible values, which is a parallelepiped in an n_τ-dimensional Euclidian space. We will denote this feasible set as $\bar{U}$. During the DSP, bounds (28) together with constraints (32) and (33) prescribed for complementary control variables $u_{7+j} \equiv \lambda_j (j \leqslant n_\lambda, n_\lambda = 2 \text{ or } 3)$ define, in an $(n_\tau + n_\lambda)$-dimensional Euclidian space, a set with polyhedral geometry which has right and oblique faces. It is a time-dependent convex polytope in which the above criterion (35) must be minimized. We will label this feasible set $U(t)$, in which optimal control $\boldsymbol{u}$ has to be found during the DSP.

5.2. State-Unconstrained Optimal-Control Problem

Dealing directly with state inequality constraints such as eqs. (26) and (27), using the PMP, leads to quite involved non-smooth optimal conditions (Pontryagin et al. 1962; Ioffe and Tihomirov 1979) that make the optimal control problem practically unsolvable. An alternative approach is to implement a penalty technique. This resembles methods used to solve mathematical programming problems. An exterior penalty method, as used in Chessé and Bessonnet (2001) and Bessonnet, Chessé, and Sardain (2002), is easy to implement, and proved to be computationally efficient. It consists of minimizing the integral amount of the constraints wherever they are an infringement. To that end, let us group together inequality state constraints (26) and (27) in the vector-valued function $\mathbf{C}^S(\mathbf{x}(t))$ such that

$$\mathbf{C}^S = (C_1^S, ..., C_{n_S}^S)^T, (n_S \geqslant 8).$$

Then, setting

$$t \in [t^i, t^f], \ C_i^{S+}(\mathbf{x}(t)) = \text{Max}(0, \ C_i^S(\mathbf{x}(t)));$$

$$\mathbf{C}^{S+} = (C_1^{S+}, ..., C_{n_S}^{S+})^T,$$

we define the quadratic penalty function ψ_S such that

$$\psi_S(\mathbf{x}) = \tfrac{1}{2}[\mathbf{C}^{S+}(\mathbf{x})]^T \mathbf{D}_S \mathbf{C}^{S+}(\mathbf{x}). \qquad (36)$$

Moreover, we deal with state equality constraints (14) using a similar approach, by introducing the second penalty function

$$t \in [t^i, t^f], \ \psi_h(\mathbf{x}(t)) = \tfrac{1}{2}[\mathbf{C}_h(\mathbf{x}(t))]^T \mathbf{D}_h \mathbf{C}_h(\mathbf{x}(t)). \quad (37)$$

In eqs. (36) and (37), $\mathbf{D}_S$ and $\mathbf{D}_h$ denote diagonal weighting matrices. Both of the above functions will be minimized by considering the augmented criteria

$$J_{SS}^*(\bar{\mathbf{u}}) = J_{SS}(\bar{\mathbf{u}}) + r_S \int_{t^i}^{t^f} \psi_S(\mathbf{x}(t))\,dt \qquad (38)$$

$$J_{DS}^*(\mathbf{u}) = J_{DS}(\mathbf{u}) + \int_{t^t}^{t^f} [r_S \psi_S(\mathbf{x}(t)) + r_h \psi_h(\mathbf{x}(t))]\,dt \quad (39)$$

where r_S and r_h are penalty factors. In theory, it can be shown that penalty functions vanish through the minimization of the cost function when penalty factors tend towards infinity (Lele and Jacobson 1969). In fact, reasonably high given values will enable the penalty functions to have negligible residual values. The reader is referred to the beginning of Section 7 for numerical examples.

At this point, the state-unconstrained optimal-control problem we intend to solve can be summarized as follows

for r_S great, $\begin{cases} \underset{\bar{u}\in\bar{U}}{\text{minimize}} \ J_{SS}^*(\bar{\mathbf{u}}), & (40) \\ \text{and } r_h \text{ great, } \underset{u\in U(t)}{\text{minimize}} \ J_{DS}^*(\mathbf{u}), & (41) \end{cases}$

while satisfying the state equations

$$t \in [t^i, t^t], \quad \dot{\mathbf{x}}(t) = \bar{\mathbf{F}}(\mathbf{x}(t), \bar{\mathbf{u}}(t)), \tag{42}$$

$$t \in [t^t, t^f], \quad \dot{\mathbf{x}}(t) = \mathbf{F}(\mathbf{x}(t), \mathbf{u}(t)), \tag{43}$$

together with either the boundary constraints

$$k = 1, \ ..., \ 4 \ \left\{ \begin{array}{l} C_k^i(\mathbf{x}_L(t^i)) = 0 \\ C_k^t(\mathbf{x}_L(t^t)) = 0 \\ C_k^f(\mathbf{x}_L(t^f)) = 0 \end{array} \right. \tag{44}$$

or the boundary conditions

$$\left\{ \begin{array}{l} \mathbf{x}_L(t^i) = \mathbf{x}_L^i \\ \mathbf{x}_L(t^t) = \mathbf{x}_L^t \\ \mathbf{x}_L(t^f) = \mathbf{x}_L^f \end{array} \right. . \tag{45}$$

In the latter case, $\mathbf{x}_L^i$, $\mathbf{x}_L^t$, and $\mathbf{x}_L^f$ denote given values.

As we want to optimize both step phases separately, the above problem will be split into two independent optimization problems set on the intervals of time $[t^i, t^t]$ and $[t^t, t^f]$ of the SSP and DSP of the gait, respectively.

6. Solving a Two-Point Boundary Value Problem

The presentation is focused on the DSP which adds to the characteristics of the SSP, quite restrictive geometric and sthenic closure conditions. Nevertheless, both problems as stated in eqs. (40), (41) and (42), (43), each being completed with conditions (44) or (45), are formally identical. Indeed, differences between the two problems, due to additional terms appearing in the second, expand when deriving necessary conditions of optimality stated by the PMP.

The reader is referred to textbooks and monographs such as Pontryagin et al. (1962), Ioffe and Tihomirov (1979), and Lewis and Syrmos (1995) for details concerning the formulation of the PMP. In fact, as the final optimal control problem we have to deal with is unconstrained in the state, optimality conditions are formally quite easy to derive.

We assume that constraints (44) are solved in the state $\mathbf{x}_L$ through relationships (21)–(24). Therefore, we take only boundary conditions (44) into consideration. In this way, the optimization problem to be solved consists of determining a state vector-function $t \to \mathbf{x}(t)$ and a control vector-function $t \to \mathbf{u}(t) \in U(t)$ minimizing the augmented criterion (41), while satisfying the state equation (43) together with the boundary conditions (45).

Setting

$$L(\mathbf{x}, \mathbf{u}) = \mathbf{u}^T \mathbf{D}_u \mathbf{u} + r_S \psi_S(\mathbf{x}) + r_h \psi_h(\mathbf{x})$$

for the Lagrangian of criterion J_{DS}^* in eq. (39), and defining the Hamiltonian function

$$\mathbf{w} \in \Re^{n_q}, \quad H(\mathbf{x}, \mathbf{u}, \mathbf{w}) = \mathbf{w}^T \mathbf{F}(\mathbf{x}, \mathbf{u}) - L(\mathbf{x}, \mathbf{u}),$$

the PMP states that, if $t \to (\mathbf{x}(t), \mathbf{u}(t))$ is a solution of eqs. (42), (43), and (45), then a $2n_q$-vector adjoint function $t \to \mathbf{w}(t)$ exists such that $t \to (\mathbf{x}(t), \mathbf{u}(t), \mathbf{w}(t))$ satisfies the adjoint equation

$$t \in [t^t, t^f], \quad \dot{\mathbf{w}}(t) = -(\partial H / \partial \mathbf{x})^T$$

$$\equiv -(\partial \mathbf{F} / \partial \mathbf{x})^T \mathbf{w} + (\partial L / \partial \mathbf{x})^T \tag{46}$$

and the maximality condition of the Hamiltonian

$$t \in [t^t, t^f], \quad H(\mathbf{x}(t), \mathbf{u}(t), \mathbf{w}(t)) = \underset{v \in U(t)}{\text{Max}} \ H(\mathbf{x}(t), \mathbf{v}, \mathbf{w}(t)). \tag{47}$$

Condition (47) plays a key role in dealing with the control vector $\boldsymbol{u}$. It allows $\boldsymbol{u}$ to be expressed, at every time t, as a function of both the state and the co-state vector variables $\boldsymbol{x}$ and $\boldsymbol{w}$, that is $\mathbf{u}(t) = \mathbf{U}(\mathbf{x}(t), \mathbf{w}(t))$. Substituting this expression for $\boldsymbol{u}$ in state and co-state equations (43) and (46) yields the $4n_q$-order differential system

$$t \in [t^t, t^f], \quad \left\{ \begin{array}{l} \dot{\mathbf{x}}(t) = \mathbf{F}^*(\mathbf{x}(t), \mathbf{w}(t)) \\ \dot{\mathbf{w}}(t) = \mathbf{G}^*(\mathbf{x}(t), \mathbf{w}(t)) \end{array} \right., \tag{48}$$

in which the state variable $\boldsymbol{x}$ must satisfy the $4n_q$ end conditions

$$\left\{ \begin{array}{l} \mathbf{x}(t^t) = \mathbf{x}^t \\ \mathbf{x}(t^f) = \mathbf{x}^f \end{array} \right. \tag{49}$$

derived from eq. (45).

The two-point boundary value problem (48), (49) can be solved using existing algorithms. The numerical techniques we use are described in Bessonnet, Sardain, and Chessé (2002). The method involves solving the problem in two stages. In the first stage, we are searching for a guess solution by implementing an easy-to-use shooting method described in Bryson and Ho (1975), and based on the construction of a transition matrix algorithm. As this technique lacks numerical robustness, the problem is solved with null penalty factors r_S and r_h, these giving rise to some stiff numerical conditioning. In the second stage, the problem is solved iteratively for increasing values of r_S and r_h using the routine D02RAF of the NAG FORTRAN Library, which implements a finite-difference algorithm. This computing code is quite efficient, and withstands sufficiently high values of penalty factors for having non-significant final residual values of both penalty functions.

7. Generating an Optimal Walking Sequence

In this section we present results concerning the construction of a walking sequence on level ground. This comprises starting, cyclic, decelerating, and stopping steps. Computations were carried out on the basis of numerical data given in Table 1. These data represent the mechanical characteristics

Table 1. Mechanical Design Parameters of the Biped BIP (Figure 5)

Link L_i	L_1	L_2	L_3	L_4	L_5	L_6	L_7
Length r_i (m)	0.188	0.410	0.410	0.410	0.410	0.290	0.146
Mass m_i (kg)	2.340	6.110	10.900	10.900	6.110	2.340	66.110
a_i (m)	0.143	0.258	0.250	0.160	0.152	0.045	0.391
b_i (m)	0.042	0.028	0.005	−0.005	−0.028	−0.042	0.029
I_i (m²kg)	0.100	0.690	1.310	1.020	0.720	0.070	18.990

Centers of gravity are defined by setting $O_iG_i = a_i\mathbf{x}_i + b_i\mathbf{y}_i$ (Figure 1), $\mathbf{x}_i = O_iO_{i+1}/r_i$, $\mathbf{y}_i = \mathbf{z}_0 \times \mathbf{x}_i$. I_i refers to the moment of inertia of link L_i about O_i.
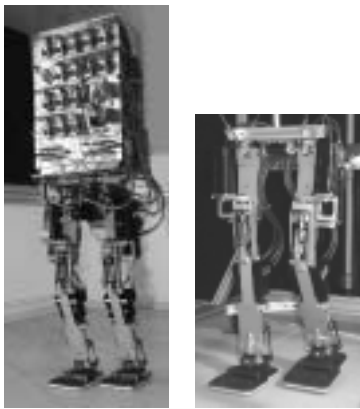
Fig. 5. The biped BIP and its locomotion system: 15 degrees of freedom, 1.8 m, 107 kg (LMS, University of Poitiers, and INRIA- R.A., France).

Fig. 6. Cyclic optimal step (sagittal DSP and SSP) of the biped BIP.

of the biped BIP (Figure 5) when considered to be moving in its sagittal plane. A cyclic step is first presented because its transition kinematic characteristics are required to define starting and stopping steps.

Penalty factors r_S and r_h introduced in eqs. (38) and (39) were set at 150. It should be noted that the residual distance from the position of point A_6^t computed on the basis of closure constraints (3) and (4) to its assigned position never exceeds 0.3 mm.

7.1. Cyclic Step

A purely cyclic step is defined (as described in Section 4.1) by conditions (18) and (19), together with the swapping relationships (21) and (22) at the end of the cycle. Such conditions need some complementary data. Walk speed is the most significant one. In the simulation presented here, it is equal to 0.75 m s^{-1} (2.7 km h^{-1}), which represents a fairly fast walk. After a few numerical tests, the corresponding step length was set at 0.5 m, while the motion time of the DSP was set at 0.25% of the total cycle time.

A stick diagram of the optimal motion is shown in Figure 6. The gait pattern has particular characteristics. First, the legs
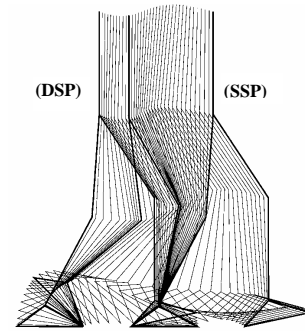
are slightly flexed in order for the foot of the stance leg to remain flat on the ground during the whole swing phase. Secondly, at the end of the swing phase, heel-touch takes place without impact. These two specific features are expected to ensure safer control of gait.

In Figure 7, actuating torques show few variations and remain at fairly moderate values (T_{ij} is the torque exerted by link L_i ($i = 2, \ldots, 7$) on link $L_j (j = 1, \ldots, 6)$). Although the ground contact conditions represent very restrictive constraints, time charts of ground interaction forces in Figure 8 show they are perfectly fulfilled. During both phases, all normal components of the contact forces are positive. Moreover, normal components NB1 and NA6B6 (NA6B6 is a short notation for NA6+NB6) during the double support, and normal components NA6 and NB6 during the single support, cross each other during their respective phases. This indicates that there is a steady transfer of the biped weight forward. Note also that the horizontal components, TAB1 and TAB6, never exceed 20% of normal ones. Therefore, little grip on the ground is needed to avoid sliding. It can be seen also that, at the beginning of the double support, the biped lifts its weight off the ground. Conversely, at the beginning of the single support, there is an increase in the normal supporting force as the hip rises.

In Figure 9, note that the seventh joint velocity V(L6/gd), referring to the rotation rate of link L6 versus the ground, is
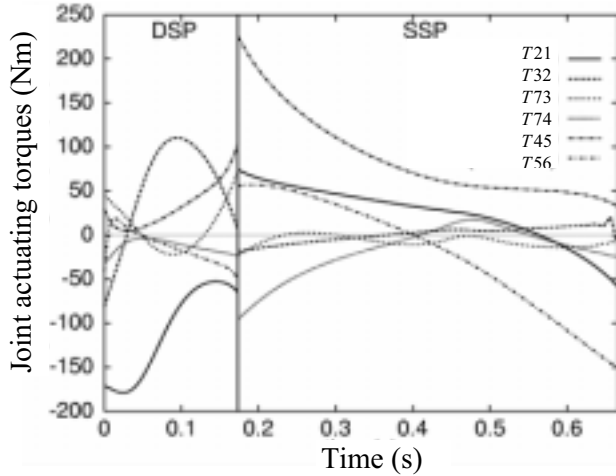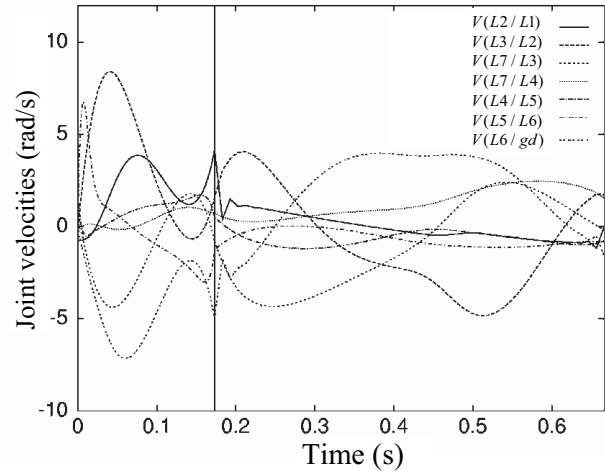
Fig. 7. Time charts of actuating torques.
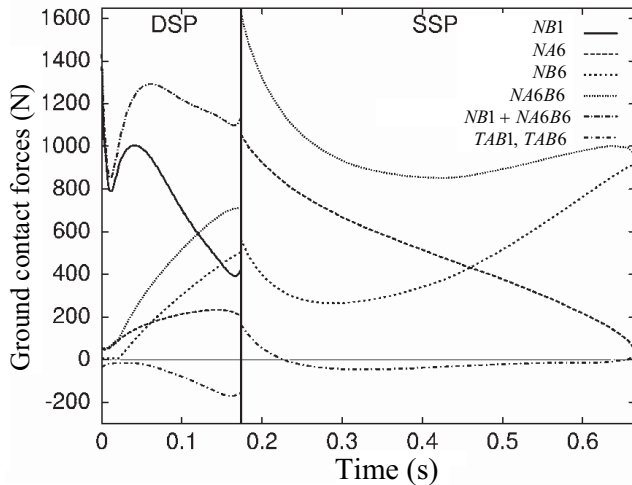

Fig. 9. Time charts of joint velocities.

Fig. 8. Time charts of ground–foot contact forces.

front foot (labeled V(L2/L1)) has sharp transitional varia-
tions between double and single supports. Such variations are
transmitted to V(L6/gd) as defined above through the term
V(L2/L1).

7.2. Starting Step

At starting time, the biped is standing with its heels together. It
performs half a step forward (Figure 10). Its final state initiates
directly the cyclic step, described immediately above. Thus,
the specified walking velocity (0.75 m s^{-1}) is reached at hip
level at the end of the step. This condition requires significant
actuating torques at ankle and knee level of the stance leg, as
shown in Figure 11. As a consequence, the stance foot exerts
a strong impulse on the ground at the beginning of the step
(Figure 12). As observed during the cyclic step, the crossed
variations of normal forces, labeled NA1 and NA2, indicate
that there is a quite regular transfer of the biped weight toward
the tip of the foot.

7.3. Stopping Step

The biped slackens its pace slightly during the double sup-
port (Figure 13) and stops at the end of the forward half sin-
gle support (Figure 14). Variations of joint actuating torques
(Figure 15) and ground contact forces (Figure 16) are quite
similar to their counterparts shown during the double support
of the cyclic step.

The ending movement (Figure 14) is initiated using the
final state of the previous DSP, where hip velocity was set
at 0.65 m s^{-1} (reduced from 0.75). The biped stops with feet
put together flat on the ground. The deceleration is fast. Cor-
relatively, actuating torques exerted at ankle and knee of the
stance leg take important values at beginning and end of the

plotted during the single support in order to ensure its contin-
uation after the double support. However, in the former case,
this rotation rate has to be seen as the linear combination of
other joint velocities, i.e.,

$$V(L6/gd) = V(L6/L5) + V(L5/L4) + V(L4/L7) + V(L7/L3) +$$
$$V(L3/L2) + V(L2/L1) + V(L1/gd).$$

During the single support, V(L1/gd) = 0. Therefore, using
the notations in Figure 8, we arrive in the end at

$$V(L6/gd) = V(L2/L1) + V(L3/L2) + V(L7/L3) - V(L7/L4) -$$
$$V(L4/L5) - V(L5/L6).$$

Joint velocities are continuous at transition between both
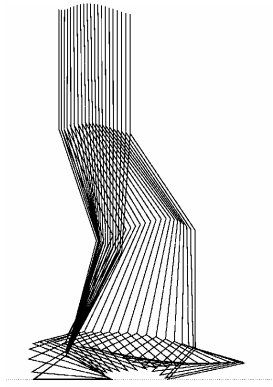phases. Nevertheless, the joint velocity at the ankle of the

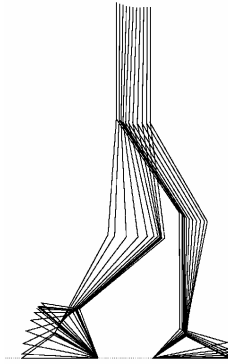Fig. 10. Starting step initiating a cyclic step.
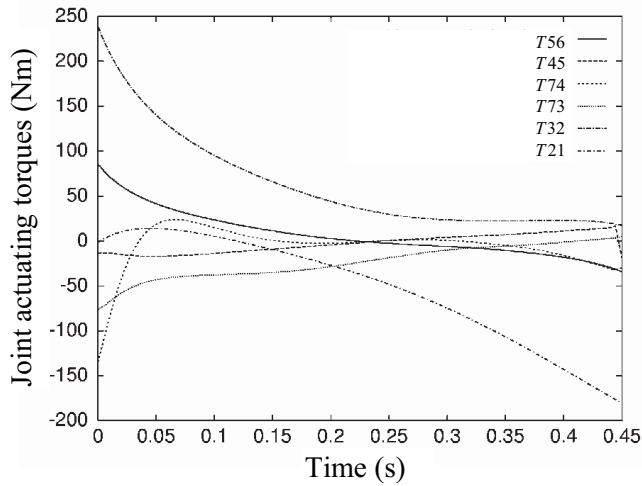

Fig. 13. Decelerating DSP.
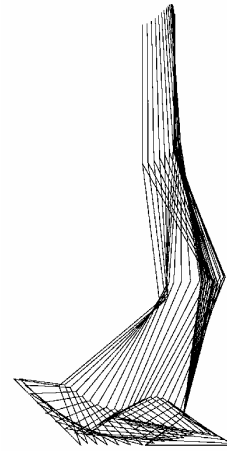

Fig. 11. Time charts of actuating torques.
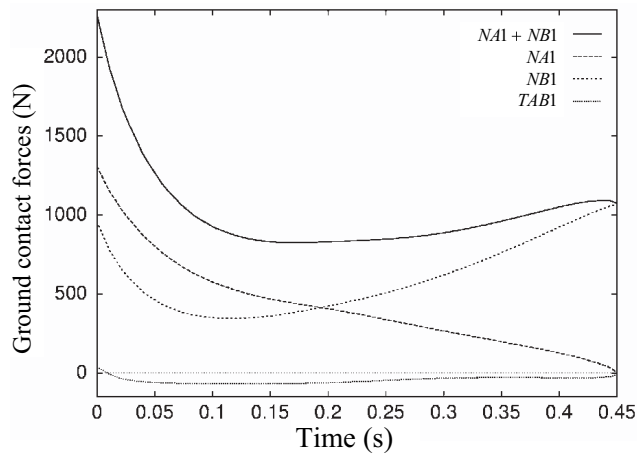

Fig. 14. Stopping SSP.

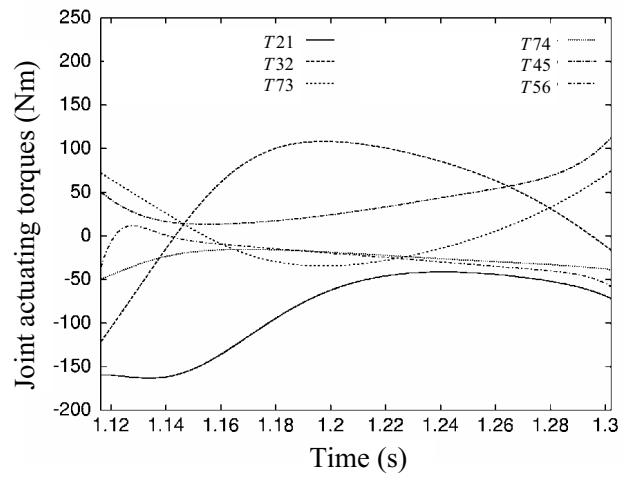Fig. 12. Time charts of ground–foot contact forces.
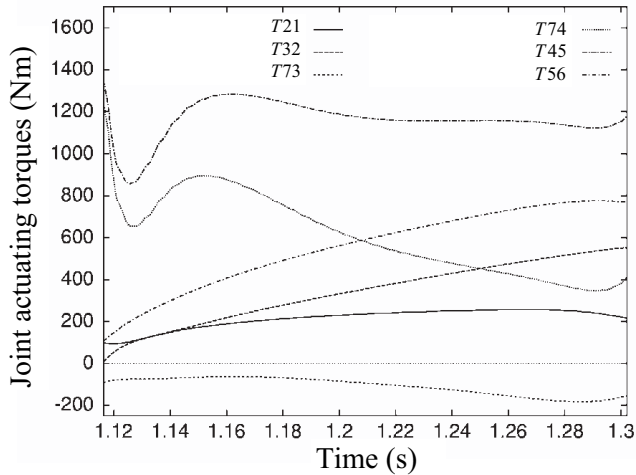

Fig. 15. Time charts of actuating torques.

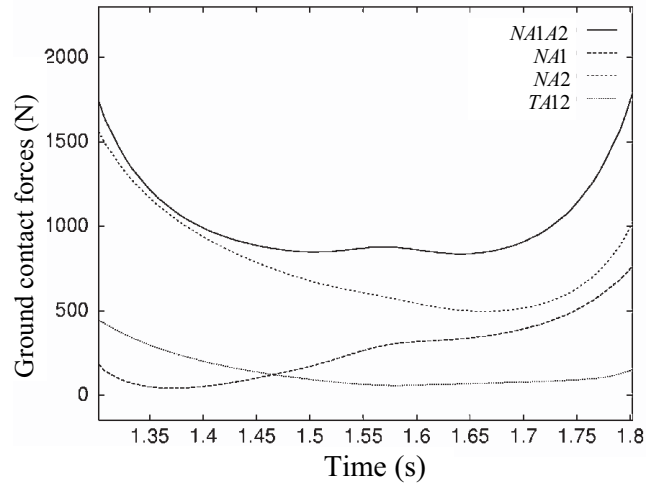Fig. 16. Time charts of ground–foot contact forces.

Fig. 18. Time charts of ground–foot contact forces.
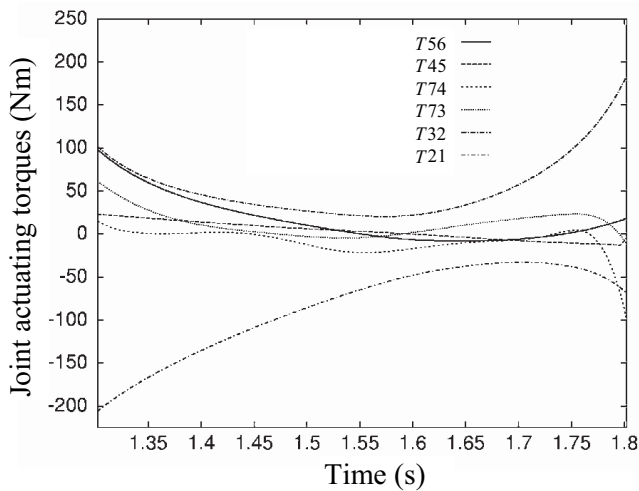

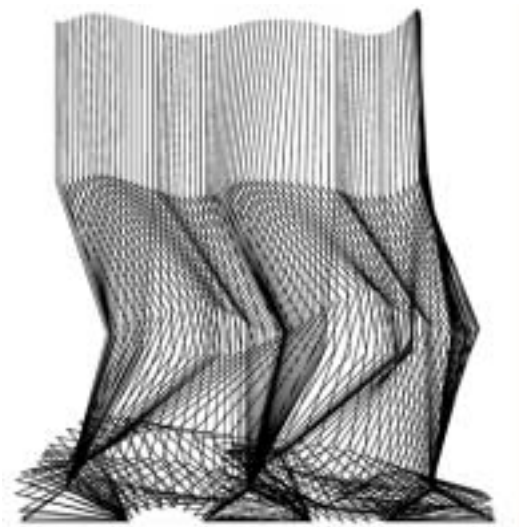Fig. 17. Time charts of actuating torques.

Fig. 19. Optimal walking sequence comprising starting, cyclic, and stopping steps.

movement (Figure 17). Similarly, the normal ground reaction force (Figure 18) shows high values at the same moments as above. We can see that the system of two forces NA1 and NA2 applied at the ends of the sole, and equivalent to uniformly distributed normal interaction forces, ends with values close to each other. This result shows that the biped is statically well balanced after stopping.

The four motions described above are assembled in the walking sequence shown in Figure 19. We can observe that the trunk leans forward slightly, especially during the cyclic and stopping steps.

7.4. Energetic Cost

The energy expended during each elementary movement was computed using

$$E = \int_{t_1}^{t_2} \sum_{i=2}^{7} |\dot{\varphi}_i(t)\tau_i(t)|\, dt$$

where t_1 and t_2 are some initial and final times.

The energetic cost of the cyclic step amounts to 205.8 J (96.3 J for the only DSP). The starting step requires 81.9 J.

The stopping step needs 112.1 and 105.1 J during the double support and single support, respectively. Thus, the total amount of energy expended to create the walking sequence shown in Figure 18 is equal to 504.9 J. In addition, the power required to perform a steady walk generated on the basis of the cyclic step, amounts to 307 W. The above energetic expenditure is greater than its human counterpart during normal gait. In fact, the gait generated is not really human-like. In particular, the biped keeps its knees flexed in order to maintain its stance foot flat on the ground during swing phases. In human gait, the heel of the stance foot lifts up before the end of such phases, making the transition towards the next double support smoother. Moreover, as heel-touch takes place without impact, the biped must tightly control its swing leg at the end of the single support. On the other hand, a good means of lowering the energetic expenditure, and making the movement smooth, would be to optimize the transition states linking two successive phases. This is future work.

8. Concluding Remarks

Legged-locomotion systems perform as time-varying mechanical structures and obey quite restrictive constraints. In this respect, two specific aspects of gait require particular attention. First, there is the unilaterality of ground–foot contacts, which affects the biped equilibrium and strictly limits the set of feasible solutions. Secondly, during the DSP of bipedal gait, the biped moves as a closed-loop kinematic system. In that case, for any joint trajectories, there is a continuum of solutions in terms of joint actuating torques. This indeterminacy could yield inappropriate distribution of actuating inputs in the locomotion system. It could then be the cause of antagonistic forces exerted between legs. The most likely consequence of this would be contact loss and sliding. The paper is especially focused on this particular phase of gait. The approach developed involves opening the closed loop at ground contact level in order to formulate a simple dynamic model and to obtain direct control over the contact forces. Indeed, the latter, especially horizontal grip forces, are considered as complementary control variables. This helps the process of finding optimal inputs directly compatible with non-sliding conditions. Closure conditions are taken into account simply through the minimization of a penalty function. In this way, the problem stated for generating optimal DSPs is formally quite similar to their SSP counterparts.

The approach presented may be completed considering various aspects of the optimization problem. First, postural configurations of the biped at transition between successive phases could be optimized in order to obtain smoother and less energy-consuming gait cycles. Secondly, dividing the SSP into two subphases in order to allow the stance foot to rotate about its tiptoe axis before heel-touch of the swing foot would contribute to smooth the transition from single support to dou-

ble support. Thirdly, gait cycles could be globally optimized. In this case, necessary optimality conditions stated using the PMP would lead to an N-point boundary value problem with $N \geqslant 3$.

Generating three-dimensional gait is not basically different from generating sagittal gait. However, due to the greater kinematic complexity, stating the optimization problem would require a great deal of effort. Furthermore, solving algorithms could be quite sensitive to this greater complexity. Nevertheless, lateral movements of three-dimensional bipeds have limited range with smooth variations during normal gait. For this reason, the numerical conditioning of stated problems might be only moderately modified.

Finally, a good challenge would be to generate optimal steps using updated constraints at every time in order to account for external disturbances. In other words, the optimization problem would be stated and solved at current time t with updated constraints to generate the finishing step. Solving such a problem in real time, as is required, seems beyond the reach of current algorithms and computers. However, if constraint disturbances are not too stiff, the solution at $t + \delta t$ will be very close to the solution at time t. The latter could be efficiently used to initiate and obtain a rapid numerical convergence toward the new solution at $t + \delta t$, and so on. Such an approach would be useful to generate and control unsteady gait of biped robots walking in a fluctuating environment.

References

Azevedo, C., Poignet, P., and Espiau, B. 2002. Moving horizon control for biped robots without reference trajectory. *Proceedings of the IEEE International Conference on Robotics and Automation (ICRA)*, Seoul, Korea, pp. 2762–2767.

Beletskii, V.-V., and Chudinov, P.-S. 1977. Parametric optimization in the problem of biped locomotion. *Mechanics of Solids* 12(1):25–35.

Bessonnet, G., Chessé, S., and Sardain, P. 2002. Generating optimal gait of a human-sized biped robot. *Proceedings of the 5th International Conference on Climbing and Walking Robots*, Paris, France, pp. 717–724.

Bessonnet, G., Sardain, P., and Chessé, S. 2002. Optimal motion synthesis – dynamic modeling and numerical solving aspects. *Multibody System Dynamics* 8:257–278.

Blajer, W., and Schiehlen, W. 1992. Walking without impacts as a motion/force control problem. *ASME Journal of Dynamic Systems, Measurement, and Control* 114:660–665.

Bryson, A.E., and Ho, Y.C. 1975. *Applied Optimal Control*, Hemisphere, New York.

Channon, P.-H., Hopkins, S.-H., and Pham, D.-T. 1992. Derivation of optimal walking motions for a bipedal walking robot. *Robotica* 10:165–172.

Chessé, S., and Bessonnet, G. 2001. Optimal dynamics of constrained multibody systems. Application to bipedal walking synthesis. *Proceedings of the IEEE International*

Conference on Robotics and Automation (ICRA), Seoul, Korea, pp. 2499–2505.

Chevallereau, C., and Aoustin, Y. 2001. Optimal reference trajectories for walking and running of a biped robot. *Robotica* 19:557–569.

Chow, C.-K., and Jacobson, D.-H. 1971. Studies of human locomotion via optimal programming. *Mathematical Biosciences* 10:239–306.

Espiau, B., and Sardain, P. 2000. The anthropomorphic biped robot BIP 2000. *Proceedings of the IEEE International Conference on Robotics and Automation (ICRA)*, San Francisco, CA, pp. 3997–4002.

Fujimoto, Y., Obata, S., and Kawamura, A. 1998. Robust biped walking with active interaction control between foot and ground. *Proceedings of the IEEE International Conference on Robotics and Automation*, Leuven, Belgium, pp. 2030–2035.

Hirai, K., Hirose, M., and Takenaka, T. 1998. The development of Honda humanoid robot. *Proceedings of the IEEE International Conference on Robotics and Automation (ICRA)*, Leuven, Belgium, pp. 160–165.

Inoue, K., Yoshida, H., Arai, T., and Mae, Y. 2000. Mobile manipulations of humanoids – real-time control based on manipulability and stability. *Proceedings of the IEEE International Conference on Robotics and Automation (ICRA)*, San Francisco, CA, pp. 2217–2222.

Ioffe, A.-D., and Tihomirov, V.-M. 1979. *Theory of Extremal Problems,* North-Holland, Amsterdam.

Kiriazov, K. 2002. Learning robots to walk dynamically – biological control concepts. *Proceedings of the 5th International Conference on Climbing and Walking Robots*, Paris, France, pp. 3–10.

Lele, M.-M., and Jacobson, D.-H. 1969. A proof of the convergence of the Kelley–Bryson penalty function technique for state-constrained control problem. *Journal of Mathematical Analysis and Application* 26:163–169.

Lewis, F.-L., and Syrmos, V.-L. 1995. *Optimal Control,* Wiley, New York.

Löffler, K., Gienger, M., and Pfeiffer, F. 2002. Trajectory control of a biped robot. *Proceedings of the 5th International Conference on Climbing and Walking Robots*, Paris, France, pp. 437–444.

Martin, B.-J., and Bobrow J.-E. 1999. Minimum-effort motions for open-chain manipulators with task-dependent end-effector constraints. *International Journal of Robotics Research* 18(2):213–224.

Muraro, A., Chevallereau, C., and Aoustin, Y. 2003. Optimal trajectories for a quadruped robot with trot, amble and curvet gaits for two energetic criteria. *Multibody System Dynamics* 9:39 –62.

Plestan, F., Grizzle, J.-W., Westervelt, E.-R., and Abba, G. 2003. Stable walking of a 7-DOF biped robot. *IEEE Transactions on Robotics and Automation* 19(4):653 –668.

Pontryagin, L., Boltiansky, V., Gamkrelitze, A., and Mishchenko, E. 1962. *The Mathematical Theory of Optimal Processes,* Wiley Interscience, New York.

Rostami, M., and Bessonnet, G. 2001. Sagittal gait of a biped robot during the single-support phase, Part 2: optimal motion. *Robotica* 19:241–253.

Saidouni, T., and Bessonnet, G. 2002. Gait trajectory optimization using approximation functions. *Proceedings of the 5th International Conference on Climbing and Walking Robots*, Paris, France, pp. 709–716.

Saidouni, T., and Bessonnet, G. 2003. Generating globally optimized sagittal gait cycles of a biped robot. *Robotica* 21:199–210.

Sardain, P., Rostami, M., and Bessonnet, G. 1998. An anthropomorphic biped robot: dynamic concepts and technological design. *IEEE Transactions on Systems, Man and Cybernetics* 28A(6):823–838.

Sutherland, D.-H., Kaufman, K.-R., and Moitoza, J.-R. 1994. Kinematics of normal human gait. *Human Walking*, J. Rose and J.G. Gamble, editors, Williams and Wilkins, Baltimore, MD, pp. 23–44.

Visioli, A. 2000. Trajectory planning of robot manipulators by using algebraic and trigonometric splines. *Robotica* 18:611–631.

Vukobratovic, J., Borovac, B., Surla, D., and Stokic, D. 1990. *Biped Locomotion: Dynamics, Stability, Control and Applications*, Springer-Verlag, Berlin.